ISSN 1674-1056
http://cpb.iphy.ac.cn
http://iopscience.iop.org/cpb
中国物理 B
Chinese Physics
中国物理 Chinese Physics B

Double-rod metasurface for mid-infrared polarization conversion

Yang Pu(蒲洋), Yi Luo(罗意), Lu Liu(刘路), De He(何德), Hongyan Xu(徐洪艳), Hongwei Jing(景洪伟), Yadong Jiang(蒋亚东), Zhijun Liu(刘志军)
Citation: Chin. Phys. B . 2018, 27(2): 024202. **doi:** 10.1088/1674-1056/27/2/024202

Journal homepage: http://cpb.iphy.ac.cn; http://iopscience.iop.org/cpb

What follows is a list of articles you may be interested in

Modeling for multi-resonant behavior of broadband metamaterial absorber with geometrical substrate

Kai-Lun Zhang(张凯伦), Zhi-Ling Hou(侯志灵), Song Bi(毕松), Hui-Min Fang(房惠敏)
Chin. Phys. B . 2017, 26(12): 127802. **doi:** 10.1088/1674-1056/26/12/127802

A linear-to-circular polarization converter based on I-shapedcircular frequency selective surfaces

Jia-Liang Wu(吴家梁), Bao-Qin Lin(林宝勤), Xin-Yu Da(达新宇), Kai Wu(吴凯)
Chin. Phys. B . 2017, 26(9): 094201. **doi:** 10.1088/1674-1056/26/9/094201

Ultra-broadband and high-efficiency polarization conversion metasurface with multiple plasmon resonance modes

Guo-Xiang Dong(董果香), Hong-Yu Shi(施宏宇), Song Xia(夏颂), Wei Li(李玮), An-Xue Zhang(张安学), Zhuo Xu(徐卓), Xiao-Yong Wei(魏晓勇)
Chin. Phys. B . 2016, 25(8): 084202. **doi:** 10.1088/1674-1056/25/8/084202

Broadband perfect polarization conversion metasurfaces

Chen Hong-Ya, Wang Jia-Fu, Ma Hua, Qu Shao-Bo, Zhang Jie-Qiu, Xu Zhuo, Zhang An-Xue
Chin. Phys. B . 2015, 24(1): 014201. **doi:** 10.1088/1674-1056/24/1/014201

Wide-band circular polarization-keeping reflection mediated by metasurface

Li Yong-Feng, Zhang Jie-Qiu, Qu Shao-Bo, Wang Jia-Fu, Zheng Lin, Zhou Hang, Xu Zhuo, Zhang An-Xue
Chin. Phys. B . 2015, 24(1): 014202. **doi:** 10.1088/1674-1056/24/1/014202

Double-rod metasurface for mid-infrared polarization conversion*

Yang Pu(蒲洋)[1], Yi Luo(罗意)[1], Lu Liu(刘路)[1], De He(何德)[1], Hongyan Xu(徐洪艳)[2], Hongwei Jing(景洪伟)[2], Yadong Jiang(蒋亚东)[1], and Zhijun Liu(刘志军)[1,†]

[1] *School of Optoelectronic Information, University of Electronic Science and Technology of China, Chengdu* 610054, *China*

[2] *Institute of Optics and Electronics, Chinese Academy of Sciences, Chengdu* 610209, *China*

(Received 26 July 2017; revised manuscript received 16 October 2017; published online 5 January 2018)

Resonant responses of metasurface enable effective control over the polarization properties of lights. In this paper, we demonstrate a double-rod metasurface for broadband polarization conversion in the mid-infrared region. The metasurface consists of a metallic double-rod array separated from a reflecting ground plane by a film of zinc selenide. By superimposing three localized resonances, cross polarization conversion is achieved over a bandwidth of 16.9 THz around the central frequency at 34.6 THz with conversion efficiency exceeding 70%. The polarization conversion performance is in qualitative agreement with simulation. The surface current distributions and electric field profiles of the resonant modes are discussed to analyze the underlying physical mechanism. Our demonstrated broadband polarization conversion has potential applications in the area of mid-infrared spectroscopy, communication, and sensing.

Keywords: metasurface, polarization conversion, mid-infrared, broadband

PACS: 42.25.Ja, 78.67.Pt, 95.85.Hp **DOI:** 10.1088/1674-1056/27/2/024202

1. Introduction

Due to the presence of several unique electromagnetic phenomena, such as thermal radiation, molecular fingerprint absorption, and atmospheric transmission, the mid-infrared region with wavelengths ranging from 2 μm to 30 μm is of particular interest for both fundamental and applied studies.[1] Significant progress has been made in the past decades for mid-infrared components, especially on lasers,[2,3] detectors,[4,5] and modulators.[6] In order to develop the mid-infrared technology to its full capacity, new device functionalities need to be developed, which depend critically on the material and structural designs.

Polarization is one of the fundamental properties of electromagnetic waves. Control of the polarization state of mid-infrared lights is important for a wide range of applications such as spectroscopy, wireless communication, and molecular sensing.[7] Conventional polarization control has been realized by employing the Brewster effect or birefringence,[8] which usually requires a relatively long optical path to obtain sufficient phase accumulation. Recently, artificial materials such as optical antennas and metamaterials have emerged as a promising approach to manipulate the polarization of lights.[9–11] A large number of high performance polarization converters have been reported at microwave and terahertz frequencies using various metasurface designs,[12–18] which are typically based on metal–insulator–metal (MIM) layered structures. In order to realize similar device functionality in the infrared region with higher frequencies, one would meet the challenge of smaller device features in fabrication, and need to take into account the non-perfect conducting properties of metals.[19,20] Despite the fact that many metamaterial structures, such as the plasmonic optical antennas and graphene-based metasurfaces, have been proposed for polarization conversion in theory,[21–25] there are only a few experimental demonstrations in the infrared region. Lévesque *et al.* presented a plasmonic L-shaped antenna which converts the linear polarization of light to its cross direction in the mid-infrared region.[26] Recently, Zhang *et al.* demonstrated a near-infrared polarization converter using an ellipse-shaped plasmonic metasurface.[27] Both of these infrared polarization converters are based on two overlapped plasmonic resonances. In order to increase the device's bandwidth as desirable in practical applications, one pathway is to superimpose more resonant modes.

In this paper, we demonstrate a mid-infrared polarization converter by superimposing three resonances in a double-rod metasurface. The double-rod metamaterials have been well investigated in prior studies with focuses on several fundamental aspects such as collective effects, plasmon-induced transparency, and dark and bright mode properties, etc.[28–30] Here, we report on the effect of polarization conversion in a double-rod metasurface. By fabricating a metasurface made of a gold double-rod array atop a dielectric film backed with a metallic ground plane, we measured a cross polarization conversion over a bandwidth of 16.9 THz around the central frequency at 34.6 THz with conversion efficiency exceeding 70%. The sur-

*Project supported by the National Natural Science Foundation of China (Grants Nos. 61421002 and 61575036), the Chinese National 1000 Plan for Young Talents, and the Startup Funding from University of Electronic Science and Technology of China.

†Corresponding author. E-mail: liuzhijun@uestc.edu.cn

© 2018 Chinese Physical Society and IOP Publishing Ltd

face current distributions and electric field profiles of relevant resonant modes are investigated to reveal the mechanism of the reflective polarization conversion. Our demonstrated double-rod metasurface exhibits more operating bands as compared to previous designs.

2. Design and fabrication

The unit-cell of our designed metasurface structure is sketched in Fig. 1(a), made of a bottom copper ground plane, a dielectric ZnSe film, and top metallic double rods. The geometrical parameters of the unit-cell are designed as $p = 3$ μm, $l_1 = 2$ μm, $l_2 = 1.5$ μm, $h = 0.72$ μm, and gap $= 0.2$ μm. The double rods are located at the center of the unit-cell and orientated 45° from the x and y directions. To fabricate the designed metasurface, we first evaporated a 300-nm thick Cu film on a silicon substrate to serve as the ground plane, and then grew a 0.72-μm thick ZnSe film on top of the Cu using an e-beam evaporation technique. Finally, a gold double-rod array was fabricated on top of the ZnSe with standard e-beam lithography, metal deposition and lift-off processes. Figures 1(b) and 1(c) show the scanning electron microscope (SEM) images of the fabricated sample. The area size of the metasurface is 2 mm×2 mm.

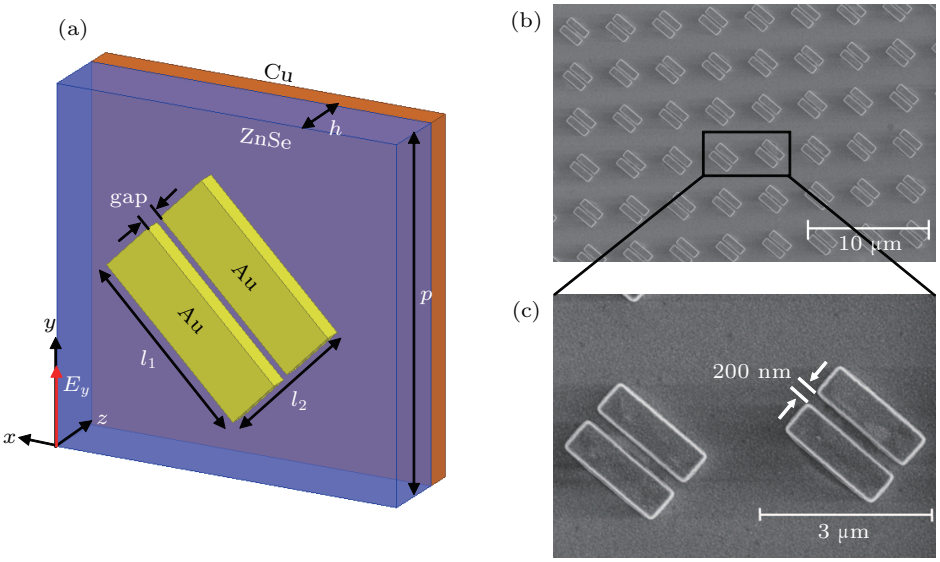


Fig. 1. (color online) (a) Unit-cell of the proposed double-rod metasurface; (b) Top-view of a large area and (c) close-up view of a small area of the fabricated sample under scanning electron microscope. The red arrow E_y represents the polarization of incident light.

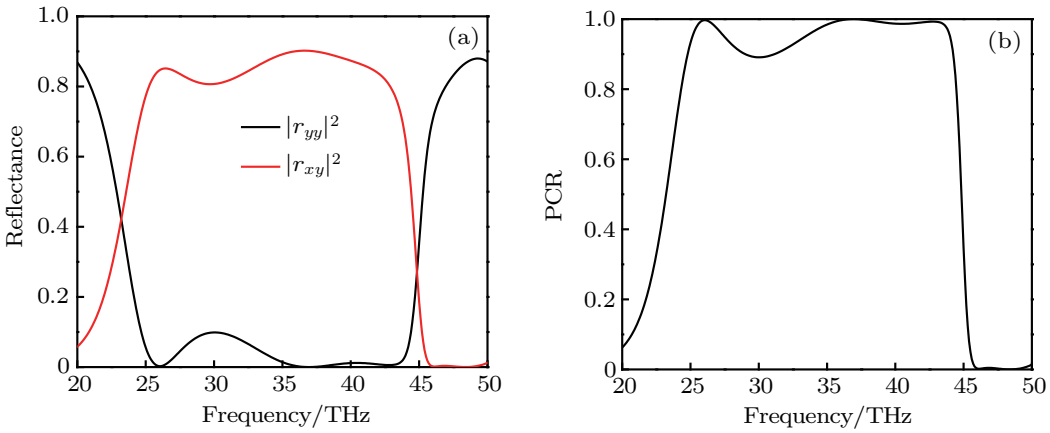


Fig. 2. (color online) (a) Simulated reflectance and (b) PCR of the proposed double-rod metasurface at normal incidence.

The structure is modeled and simulated with Ansys' HFSS solver in driven mode, which is based on the finite element method in frequency domain. The Cu and Au layers are described with a Drude model with optical parameters given in Ref. [31]. The dielectric constant of the spacer ZnSe layer is assumed to be 2.4 as given in Ref. [32]. Floquet excitation port and periodic boundary condition were applied in the unit-cell, and the S parameters were used to calculate the complex reflection coefficients. The incident light is assumed to be polarized in the y direction, and the reflection coefficients of the cross-polarized and co-polarized lights are designated as r_{xy} and r_{yy}, respectively. The polarization conversion ra-

tio (PCR) is defined as PCR $= r_{xy}^2/\left(r_{xy}^2+r_{yy}^2\right)$.[21] Figure 2(a) shows the simulated reflectance of the proposed polarization converter at normal incidence. It is seen that within the frequency range from 24.9 THz to 44.2 THz, the cross-polarized reflectance $|r_{xy}|^2$ is larger than 0.8, while the co-polarized reflectance $|r_{yy}|^2$ is smaller than 0.1. These features of $|r_{xy}|^2$ and $|r_{yy}|^2$ indicate a function of cross polarization conversion in reflection mode. We can also observe that the co-polarized reflectance $|r_{yy}|^2$ reaches zero at frequencies of 26 THz, 37 THz, and 43.3 THz, which correspond to three resonant modes. Figure 2(b) shows the calculated PCR of the device. It is readily seen that within the frequency range from 24.9 THz to 44.2 THz, the PCR is higher than 90% and reaches close to 100% at the three resonant frequencies. This designed polarization converter exhibits a PCR with an FWHM bandwidth of 18.5 THz and peak values exceeding 90%.

3. Measurement results and analysis

The metasurface sample was characterized with Fourier transform infrared reflection (FTIR) spectroscopy. A broadband globar IR light from the FTIR spectrometer was focused by an 8-inch (1 inch = 2.54 cm) focal length off-axis parabolic mirror onto the sample with a spot size of about 1.5 mm. The reflection from a copper mirror was used as the reference spectrum. Two wire-grid polarizers were arranged in either parallel or crossed configurations in the optical path to measure the co-polarized or cross-polarized reflection spectra, respectively. The setup consisted of two coaxial sample and detector rotational stages. The blocking of incident beam by the detector limits the minimum incident angle to be 15° in our measurements.

Figure 3(a) shows the measured reflection spectra at an incident angle of 15° for incident y-polarized light. The co-polarized reflectance $|r_{yy}|^2$ is smaller than 20%, while the cross-polarized reflectance $|r_{xy}|^2$ takes considerable values up to 57% within the band of 26.2 THz to 43 THz, indicating a function of polarization conversion. These measured results are in qualitative agreement with the simulation as shown in the dashed curves. However, there is an obvious deviation between experiment and simulation. The blueshift in measured spectra is likely caused by the uncertain variations of ZnSe refractive index or thickness according to our simulations. In addition, the measured cross-polarized reflectance is much smaller than the calculated value, which we attribute to possible light scattering on the structured top surface. It is worth noting that there are some noisy spike features in the measured spectra, which are caused by fluctuations of air absorption in the characterization system. Figure 3(b) shows the measured PCR of the device, which exhibits a bandwidth of 16.9 THz around the central frequency at 34.6 THz with peak values exceeding 70%. This measured PCR is in general agreement with the simulated result as shown in the black dashed curve.

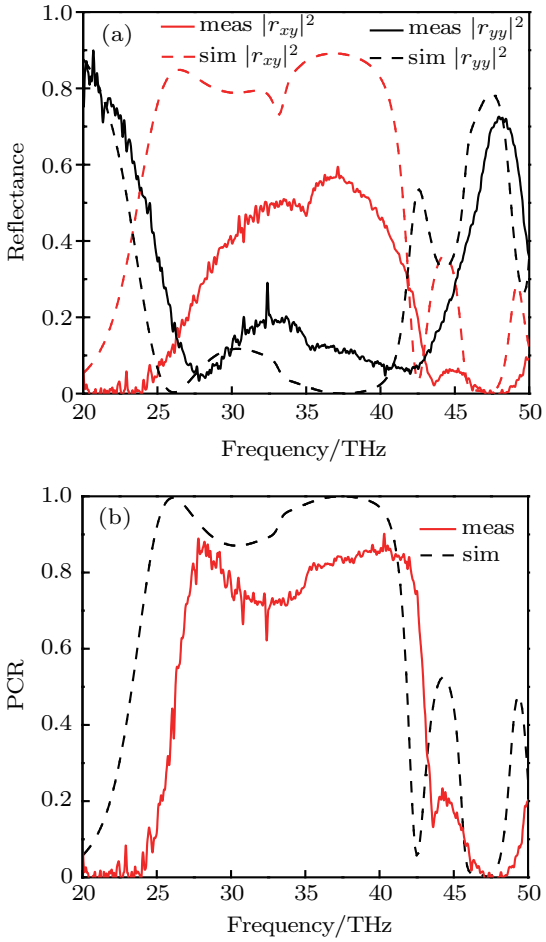


Fig. 3. (color online) Measured (meas.) and simulated (sim.) reflectance (a) and PCR (b) of the metasurface sample.

In prior reported broadband polarization converters[11,17,33] it has been shown that the physical origin of the cross polarization conversion is related to two eigenstates excited at two orthogonal incident polarizations, which are along ±45° directions with respect to the y-axis direction. Here we examined these two eigenstates in our metasurface structure. The incident polarization along +45° counterclockwise from the positive y-axis direction is defined as state A, and its orthogonal polarization along −45° counterclockwise from the positive y-axis direction is defined as state B. Figure 4(a) shows the reflection coefficients for these two states, i.e., R_{AA} and R_{BB}. It is seen that R_{AA} and R_{BB} exhibit resonances at 24.4 THz and 44.8 THz, 35.3 THz and 44.9 THz, respectively. The phase difference of R_{AA} and R_{BB} is about 180° in the frequency range from 26 THz to 43.3 THz as shown in Fig. 4(b). This phase relationship gives a clear picture of the polarization conversion in our proposed structure. Namely, the incident y-polarization can be decomposed into two orthogonal components with

polarizations along +45° and −45° counterclockwise from the positive *y*-axis direction, respectively. These two components excite the two eigenstates of *A* and *B* simultaneously. Due to the large permeability associated with the magnetic resonances,[9] a near 180° phase difference is accumulated between the two components after reflection. The recombination of these two reflected components finally results in a polarization rotation by 90° over a wide bandwidth.

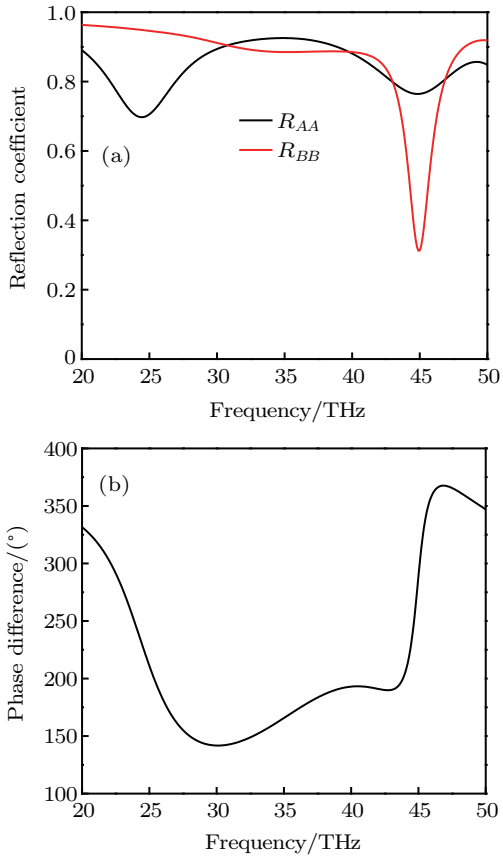


Fig. 4. (color online) (a) Simulated reflection coefficient and (b) phase difference for the two eigenstates with incident polarization of +45° and −45° counterclockwise from the positive *y*-axis direction at normal incidence.

To better understand the physical mechanism of the measured reflective polarization conversion, we investigated the properties of relevant resonant modes. Figure 5 shows the surface current distributions and electric field profiles of the three resonances at 26 THz, 37 THz, and 43.3 THz under incident *y*-polarized light at normal incidence. The arrows indicate the directions of the induced currents on front and back layers of the metasurface. We can see that the surface currents on the double-rod antenna and the bottom metal layer are antiparallel to each other, forming current loops. Therefore, the resonances at 27 THz, 37 THz, and 43.3 THz are considered as magnetic resonances. Due to the anisotropy of the metasurface, the electromagnetic wave radiated from these surface currents is polarized 45° from the incident polarization and can be decomposed into two components in the *x* and *y* directions, respectively. The *y* component accumulates a π phase shift relative to the reflected incident light, resulting in a suppressed field in the *y* polarization. The *x* component represents the converted polarization with a rotation angle of 90°. Taking the resonance of 26 THz shown in Figs. 5(a)–5(c) as an example the surface current on the top double-rod flows to the right-down corner, and the surface current on the ground plane flows to the upper-left corner. These surface currents are streaming in opposite directions and induce a magnetic field m_1 (illustrated in blue) which can be decomposed in *x* and *y* directions. The *x* component (H_{1x}) of the induced magnetic field is perpendicular to the incident electric field E_y, thus there is no cross-coupling between H_{1x} and the incident electric field E_y. However, the *y* component H_{1y} is parallel to the electric field E_y, which leads to a cross-polarization rotation with *y*-to-*x* polarization conversion. The similar physical mechanism also occurs at other two resonances at 37 THz and 43.3 THz, which are shown in Figs. 5(d)–5(f) and 5(g)–5(i), respectively. The cross-coupling effect between incident electric field E_y and the induced magnetic field in the *y* direction leads to the *y*-to-*x* polarization conversion. Namely, the incident *y*-polarized electrical field induced a parallel magnetic field component, which is accompanied with an induced electrical field in the perpendicular *x* direction, leading to the crossed polarization conversion. This mechanism of polarization conversion is similar to the ones reported in prior microwave metasurfaces.[17,18]

In addition, the electric field profiles of the resonant modes also shed light on the effects of geometric parameters on the polarization conversion performance. For the 26-THz mode shown in Fig. 5(c), its field maxima are mainly located at the edge of the structure along l_1, which suggests that the resonant frequency of this mode is expected to be inversely proportional to l_1. Similarly, the field maxima of the 37-THz mode are mostly located at the edge of the structure along l_2, which means its resonant frequency is expected to be inversely proportional to l_2. For the third mode at 43.3 THz, its field maxima are located at the corner of the unit-cell. Therefore, its resonant frequency is likely mainly determined by the periodicity *p*.

We next studied the angular dependence of the polarization conversion performance. Figures 6(a) and 6(b) show the simulated reflectance contour plots of $|r_{yy}|^2$ and $|r_{xy}|^2$ as a function of frequency and incidence angle. We can see that as the incident angle increases to up to 20°, the co-polarized reflectance $|r_{yy}|^2$ starts to increase while the cross-polarized reflectance $|r_{xy}|^2$ starts to decrease in the band around the frequency of 30 THz. Therefore, the broadband polarization conversion degrades in terms of both bandwidth and conversion efficiency when the incident angle is larger than about 20°.

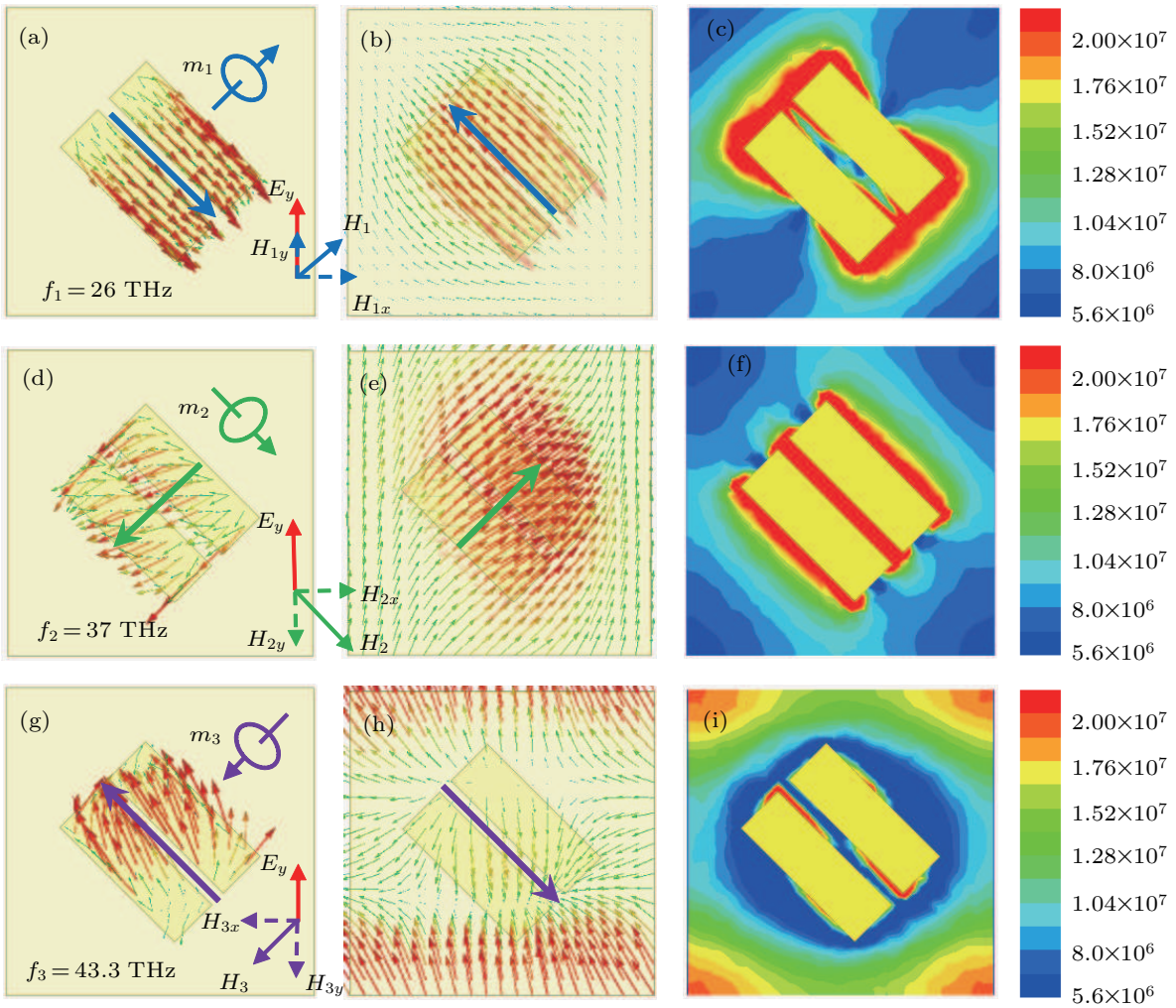


Fig. 5. (color online) Surface current distributions on the top double rods ((a), (d), (g)) and on the ground plane ((b), (e), (h)), and electrical field profiles ((c), (f), (i)) of the three resonant modes of the metasurface. Top row, middle row, and bottom row are for the resonance at 26 THz, 37 THz, and 43.3 THz, respectively.

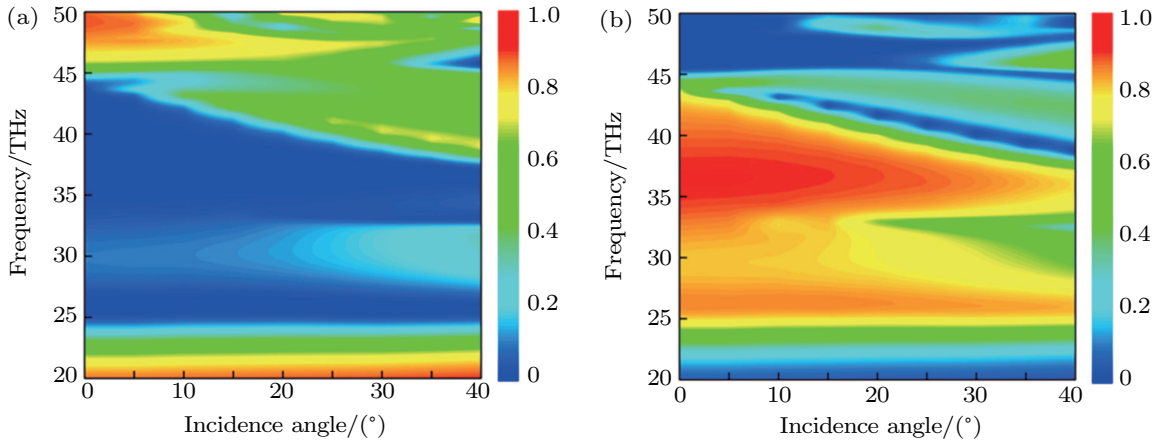


Fig. 6. (color online) Simulated (a) co-polarized reflectance $|r_{yy}|^2$ and (b) cross-polarized reflectance $|r_{xy}|^2$ of the metasurface sample as a function of frequency and incidence angle.

Finally, we examined the effect of coupling between the double rods on the polarization conversion performance. Figure 7 shows the simulated PCR of the metasurface for different gap sizes between the double rods. We can see that, as the gap increases from 0 to 200 nm, the second resonant mode at around 37 THz is excited, which leads to an increased bandwidth. As the gap size further increases beyond 200 nm, the PCR of the metasurface remains nearly unchanged. This property suggests that we could opt for a larger gap size in design to reduce the complexity in small feature fabrications while

maintaining the wide bandwidth operation.

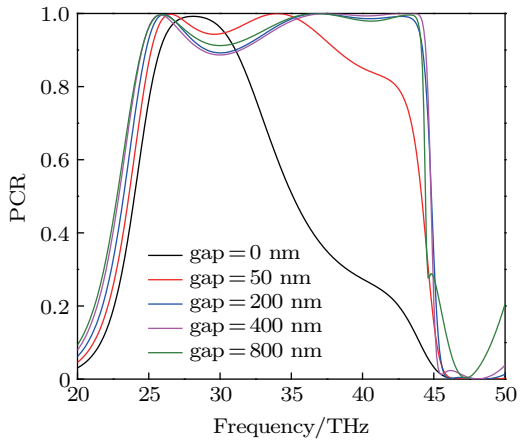


Fig. 7. (color online) PCR of the metasurface with different gap sizes between the double rods.

4. Conclusions

In conclusion, a broadband and high-efficiency reflective linear polarization converter made of double-rod metasurface has been demonstrated in the mid-infrared region both theoretically and experimentally. Our measured results have shown that the double-rod metasurface converted linearly polarized light to its cross polarization in the frequency range from 26.2 THz to 43 THz with PCR larger than 70% and an FWHM bandwidth of 16.9 THz. The physical mechanism of the achieved broadband polarization conversion was shown to originate from three resonant modes, whose surface current distributions and electric field profiles were analyzed in detail. Our demonstrated metasurface polarization converter expands the device functionality for polarization control in the mid-infrared, which can also be scaled to other spectral regions by changing the geometrical parameters in design. Although the wide bandwidth is demonstrated here by using three overlapped resonances, the principle can be applied to involve more resonances in specially designed structures for further improvements. In addition, by replacing the metallic ground place with structured antennas, we can expect unidirectional light transmission besides the polarization conversion.

References

[1] Hu J, Meyer J, Richardson K and Shah L 2013 *Opt. Mater. Express* **3** 1571
[2] Jackson S D 2012 *Nat. Photon.* **6** 423
[3] Yao Y, Hoffman A J and Gmachl C F 2012 *Nat. Photon.* **6** 432
[4] Tidrow M Z, Beck W A, Clark III W W, Pollehn H K, Little J W, Dhar N K, Leavitt R P, Kennerly S W, Beekman D W, Goldberg A C and Dyer W R 1999 *Proc. SPIE* **3629** 100
[5] Chen G, Haddadi A, Hoang A-M, Chevallier R and Razeghi M 2015 *Opt. Lett.* **40** 45
[6] Yao Y, Shankar R, Kats M A, Song Y, Kong J, Loncar M and Capasso F 2014 *Nano Lett.* **14** 6526
[7] Han D, Lee K, Jo H, Song Y, Kim M and Ahn J 2016 *Opt. Express* **24** 21276
[8] Born M and Wolf E 1999 *Principles of Optics* (Cambridge: Cambridge University Press)
[9] Hao J, Yuan Y, Ran L, Jiang T, Kong J A, Chan C T and Zhou L 2007 *Phys. Rev. Lett.* **99** 063908
[10] Hao J, Ren Q, An Z, Huang X, Chen Z, Qiu M and Zhou L 2009 *Phys. Rev. A* **80** 023807
[11] Li T, Wang S M, Cao J X, Liu H and Zhu S N 2010 *Appl. Phys. Lett.* **97** 261113
[12] Feng M, Wang J, Ma H, Mo W, Ye H and Qu S 2013 *J. Appl. Phys.* **114** 074508
[13] Cheng Y Z, Withayachumnankul W, Upadhyay A, Headland D, Nie Y, Gong R Z, Bhaskaran M, Sriram S and Abbott D 2014 *Appl. Phys. Lett.* **105** 181111
[14] Shi H Y, Li J X, Zhang A X, Wang J F and Xu Z 2014 *Chin. Phys. B* **23** 118101
[15] Wu X, Meng Y, Wang L, Tian J, Dai S and Wen W 2016 *Appl. Phys. Lett.* **108** 183502
[16] Huang Y, Yang L, Li J, Wang Y and Wen G 2016 *Appl. Phys. Lett.* **109** 054101
[17] Wu J L, Lin B Q and Da X Y 2016 *Chin. Phys. B* **25** 088101
[18] Sun H, Gu C, Chen X, Li Z, Liu L and Martín F 2017 *J. Appl. Phys.* **121** 174902
[19] Novotny L 2007 *Phys. Rev. Lett.* **98** 266802
[20] Luo Y, Ying X, Pu Y, Jiang Y, Xu J and Liu Z 2016 *Appl. Phys. Lett.* **108** 231103
[21] Ding J, Arigong B, Ren H, Zhou M, Shao J, Lin Y and Zhang H 2014 *Opt. Express* **22** 29143
[22] Ding J, Arigong B, Ren H, Shao J, Zhou M, Lin Y and Zhang H 2015 *Plasmonics* **10** 351
[23] Cheng H, Chen S, Yu P, Li J, Xie B, Li Z and Tian J 2013 *Appl. Phys. Lett.* **103** 223102
[24] Yang C, Luo Y, Guo J, Pu Y, He D, Jiang Y, Xu J and Liu Z 2016 *Opt. Express* **24** 16913
[25] Chen M, Sun W, Cai J, Chang L and Xiao X 2017 *Plasmonics* **12** 699
[26] Lévesque Q, Makhsiyan M, Bouchon P, Pardo F, Jaeck J, Bardou N, Dupuis C, Haïdar R and Pelouard J-L 2014 *Appl. Phys. Lett.* **104** 111105
[27] Zhang Z, Luo J, Song M and Yu H 2015 *Appl. Phys. Lett.* **107** 241904
[28] Mousavi S H, Khanikaev A B, Neuner B, Fozdar D Y, Corrigan T D, Kolb P W, Drew H D, Phaneuf R J, Alù A and Shvets G 2011 *Opt. Express* **19** 22142
[29] Ye Z, Zhang S, Wang Y, Park Y-S, Zentgraf T, Bartal G, Yin X and Zhang X 2012 *Phys. Rev. B* **86** 155148
[30] Omaghali N E J, Tkachenko V, Andreone A and Abbate G 2014 *Sensors* **14** 272
[31] Ordal M A, Long L L, Bell R J, Bell S E, Bell R R, Alexander R W Jr and Ward C A 1983 *Appl. Opt.* **22** 1099
[32] Ahmed S and Khawaja E E 1984 *Thin Solid Films* **112** L1
[33] Yang J and Zhang J 2011 *Plasmonics* **6** 251